ARL-PROP-R-180 AR-005-606

DEPARTMENT OF DEFENCE

DEFENCE SCIENCE AND TECHNOLOGY ORGANISATION

AERONAUTICAL RESEARCH LABORATORY

MELBOURNE, VICTORIA

Propulsion Report 180

TIME-FREQUENCY DOMAIN ANALYSIS OF HELICOPTER TRANSMISSION VIBRATION

by

B.D. FORRESTER

Approved for public release

AUGUST 1991

AR-005-606

DEPARTMENT OF DEFENCE
DEFENCE SCIENCE AND TECHNOLOGY ORGANISATION
AERONAUTICAL RESEARCH LABORATORY

Propulsion Report 180

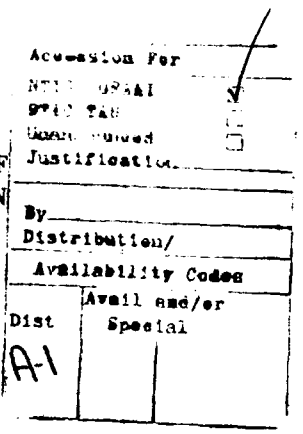

TIME-FREQUENCY DOMAIN ANALYSIS OF HELICOPTER TRANSMISSION VIBRATION

by

B.D. FORRESTER

SUMMARY

Vibration Analysis is playing an increasingly important role in the early detection of helicopter transmission faults. Current vibration analysis techniques used in helicopter transmission fault detection require selective filtering or manipulation of the signal, based on assumptions about the nature of the signal. In some cases these techniques can give misleading results. It is shown that the application of time-frequency domain representations, based on the Wigner-Ville distribution, is capable of detecting a variety of vibration features which can be used to classify faults.

POSTAL ADDRESS: **Director, Aeronautical Research Laboratory**
506 Lorimer Street, Fishermens Bend 3207
Victoria Australia

CONTENTS

1. INTRODUCTION.

Failure of helicopter transmission components can have catastrophic results and, therefore, it is vital to detect incipient failure very early. Early failure detection can lead to the scheduling of repairs with minimum disruption to the normal operations of the aircraft, bringing a saving in both cost and utility value, as well as improving the safety of the aircraft.

Vibration analysis is one method which is playing an increasingly important role in early failure detection in helicopter transmissions. Recent advances in the application of time synchronous averaging and associated enhancement techniques enable the meshing behaviour of individual gears to be examined. This allows the detection of individual tooth faults. However, it is shown that with these methods there are difficulties in determining the type and extent of tooth damage present, which can have a significant bearing on the expected time to failure of the gear.

Traditional vibration analysis methods use representations of the vibration signal in either the time or frequency domain. Neither of these representations is capable of detecting all classes of faults which may be encountered [1]. A number of analytical techniques have been devised which have proved relatively successful in the detection of certain classes of faults [2,3]. These generally require selective filtering of the time averaged signal.

A major drawback with the single domain representations is that they can accurately portray only vibration signals that are of a stationary[1] nature [4]. Although this will normally be the case for a helicopter main rotor gearbox running at nominally constant speed, the presence of most faults will cause variations in the vibration which can be viewed as short term non-stationary components. These components can be used to identify the fault.

This report examines the use of the Wigner-Ville distribution of vibration signal averages to give a representation of the signal jointly in the time and frequency domains. This allows the modulation of the signal in both time and frequency to be viewed simultaneously, enabling easy visualization of the behaviour of the signal.

A number of synthesized signals are examined to indicate how various forms of modulation are portrayed using the Wigner-Ville distribution. Practical examples

---

[1] A signal is said to be stationary if its statistical properties do not vary in time.

showing the detection of in-service faults in Wessex helicopter main rotor gearboxes and an epicyclic gearbox test rig are also presented.

2. SIGNAL AVERAGING.

In a helicopter transmission there are a large number of rotating components, all of which will contribute to the vibration signal. In order to simplify the task of analysing the vibration signal, synchronous averaging is performed for each gear shaft.

Although the transmission is operating at nominally constant speed, there will be minor speed variations in practice. For this reason, sampling of the vibration data is performed at rotational rather than time-based intervals.

The vibration is sampled at a rate which is a selected ratio of a synchronising signal from the transmission (in the case of the RAN Wessex, the generator output is used). The ratio is selected such that a fixed number of points will be sampled for each revolution of the shaft for which the signal averaging is being performed. This can be achieved either by using hardware (such as a phase-locked frequency multiplier) which generates sampling pulses at the selected ratio of the synchronising signal, or by digitally re-sampling. All examples in this paper where generated using a digital re-sampling technique where both the vibration signal and synchronising signal are sampled simultaneously using a fixed time-based sampling frequency. Cubic interpolation of the vibration signal is used to calculate the values at the required sample points, based on the phase of the synchronising signal.

The sampled vibration signal is divided into successive ensembles, each equivalent in length to exactly one revolution of the selected shaft, and the ensembles are averaged.

When a sufficient number of ensembles are averaged, noise and vibration which is not related to the selected shaft will asymptote to zero. The resultant signal average is an estimate of the vibration which is harmonically related to the selected shaft. Typically, this will be vibration at the shaft rotation frequency and its harmonics plus the tooth mesh frequencies and harmonics for each gear on the shaft.

3. PRACTICAL EXAMPLES USED.

Signal averages of the following vibration data sources are used in later sections reviewing existing vibration analysis techniques and examining the application of the Wigner-Ville distribution.

3.1 Wessex Input Pinion.

The input spiral bevel pinion of the Wessex helicopter main rotor gearbox has 22 teeth. The vibration recordings were taken from an accelerometer mounted adjacent to the input pinion. The input shaft connects the output of the engine reduction gearbox in the nose of the aircraft to the input pinion of the main rotor gearbox. The physical separation between the engine reduction gearbox and the main rotor gearbox is fairly large and, in practice, it is rare to pick up vibration from the engine or its reduction gearbox at the input pinion accelerometer. The signal average of the input shaft can therefore be assumed to contain only vibration due to the input pinion. It would be expected that this would give a vibration signal with major components at the tooth mesh frequency (22 orders) and its harmonics (n x 22).

The vibration data used here was provided from routine in-flight vibration recordings taken at the RAN Naval Air Station Nowra. Signal averages of the input pinion vibration were done at ARL during the development and testing of a computerised system for the early failure detection of Wessex input pinions.

In this report, four examples of Wessex Input Pinion signal averages have been used,

(a) an undamaged input pinion,

(b) a cracked input pinion 103 hours before failure,

(c) a cracked input pinion 42 hours before failure, and

(d) an input pinion with micro-pitting.

The signal averages for the cracked Wessex input pinion (b) and (c), were calculated from vibration recordings taken prior to an in-service failure in December 1983, which resulted in the loss of the aircraft and two lives. This crash prompted increased effort at ARL in the area of vibration analysis, including development of the techniques described in this report, in order to prevent similar failures in future.

The signal average (d) of the Wessex input pinion with severe micro-pitting (frosting) of the tooth surfaces, was calculated from vibration recordings taken 200 hours prior to removal of the pinion, also as part of the development of analysis techniques. This pinion was rejected after visual inspection prompted by high oil debris levels.

3.2 Epicyclic Test Rig Planet Gear.

An epicyclic gearbox test rig was constructed at ARL in order to develop signal averaging techniques for the extraction of vibration from individual components within epicyclic gearboxes. The gearbox has three planet gears each with 32 teeth. The examples used here are for individual planet gears, which would be expected to produce vibration signals with major components at the tooth mesh frequency (32 orders) and its harmonics (n x 32).

Two examples are used,

(a) an undamaged planet and

(b) a 'damaged' planet.

The damaged planet (b) had a simulated fault which was introduced by grinding 0.05 mm off the face of one of the teeth.

4. REVIEW OF EXISTING TECHNIQUES.

The signal average is a useful starting point for the detection of gear and/or shaft related faults. Because only a small fraction of bearing vibration is coherent with shaft rotation, the signal average has limited application to the detection of bearing faults.

It should be stressed that the signal average gives the estimated vibration not of a single gear, but of all vibration synchronous with the rotation of a shaft, which will include shaft vibration and meshing harmonics for all gears on the shaft. Vibration from any other source which happens to be synchronous with shaft rotation will also be included. For example, in the Westland Sea King helicopter the input shaft speed is exactly 3.4 times that of the main shaft, therefore vibration at 5 times input shaft speed would appear as 17 times main shaft speed (and vice versa).

In most cases, the signal average itself is not sufficient to detect faults and therefore further enhancement is required.

4.1 Figures of Merit.

Stewart [3] proposed a number of non-dimensional 'Figures of Merit', which he numbered FM0 to FM5. The 'zero-order' figure of merit FM0 was proposed as a 'fault detection filter' which detects significant change in the signal average. The higher order figures of merit were used in an attempt to identify the cause of a change detected by FM0. These cover misalignment/eccentricity (FM1), tooth breakage (FM2), wear (FM3) and 'unassignable change' (FM4 and/or FM5).

Here, we will look at two of these measures. These are FM0, the general fault detection measure, and the 'unassignable change' measure FM4.

FM0: The ratio of the peak-to-peak level of the signal average to the sum of the rms levels of the meshing components in the average. For a pure sine wave this value will be 2.828 ($4/\sqrt{2}$). Stewart suggested that a value above five would be taken as unsatisfactory.

FM4: Involves the removal of what is considered the 'regular' signal for the shaft from the signal average. The 'regular' signal typically includes the tooth meshing harmonics and possibly their upper and lower sidebands. The remaining 'residual' signal is assumed to represent the departures in the tooth meshing vibration from the average for a single gear tooth.

The kurtosis (fourth statistical moment) of the 'residual' is used as a measure of impulsive energy, and is useful for detecting localised tooth damage. The kurtosis value is 1.5 for a sine wave and 3.0 for a random signal. Typically, we would expect the values obtained to be between these values for a 'normal' gear. In practice, the limits set for the kurtosis values would normally be,

less than 3.5	- no localised damage
3.5 to 4.5	- warning level
greater than 4.5	- danger level.

4.2 Narrow Band Enhancement Technique.

It was argued by McFadden [5] that the broad band nature of the FM4 residual passes signals due to normal gear tooth pitch and profile variations as well as signals which may be due to a fault condition. It was proposed that narrow band techniques could eliminate much of the background signal, giving an improvement in sensitivity.

The narrow band enhancement technique [2] involves the narrow band filtering of the signal average about the dominant tooth meshing harmonic and removal of that meshing harmonic. The envelope of the remaining signal is then calculated. The enveloped signal can be related to the amplitude and phase modulation of the tooth meshing harmonic.

Kurtosis can be used on the enveloped narrow band signal in the same way as for the FM4 residual.

4.3 Practical Examples.

Table 1 shows the results obtained when the above methods are applied to the six practical examples described in Section 3.

	FM0 measure	FM4 (Kurtosis)	Narrow Band (Kurtosis)
Wessex Input Pinion			
Undamaged	2.52	2.71	2.69
Cracked (103 hours before failure)	3.29	4.16	7.92*
Cracked (42 hours before failure)	4.26	5.96*	4.98*
Micro-Pitting	3.01	5.60*	5.01*
Epicyclic Planet Gear			
Undamaged	2.20	2.55	2.20
Damaged	2.31	3.14	3.68

Table 1 - Results of Existing Techniques
(values indicated with * are above danger level)

None of the examples gives a value for FM0 above the suggested unsatisfactory level of five. Stewart had noted [3] that "Some problems have been encountered in its (FM0) ability to detect minor tooth damage...". It was suggested that FM4 be used as an additional test for tooth damage. Although the examples of damage here are not necessarily 'minor', they are all restricted to a localised portion of the gear. This would indicate that FM0 is not a particularly good discriminator for localised damage.

For the cracked Wessex input pinion, both the FM4 and Narrow Band techniques indicate the damage. In the early stages (at 103 hours before failure) the FM4 gives a warning level and the Narrow Band technique a danger level. At the advanced stages (42 hours before failure), the FM4 level has increased to a danger level and the Narrow Band value has decreased (though still at a danger level).

For the Wessex input pinion with micro-pitting, both the FM4 and Narrow Band techniques give values in the danger level. This is significant when compared to the results obtained for the cracked input pinion 42 hours before failure; the pinion with micro-pitting continued in service for a further 200 hours without incident whereas the cracked pinion failed within 42 hours, causing the loss of the aircraft. Thus, although the indicators are valuable in detecting the presence of a fault, they are of little value in diagnosing the type of fault or its significance

For the epicyclic planet gear, FM4 does not give an indication of the damage and the Narrow Band technique gives a warning.

4.4 Conclusions.

From the limited number of examples given above, we can make the following conclusions about these techniques:

1. The FM0 measure is of limited value for the detection of localised gear tooth faults.

2. Both the FM4 and Narrow Band measures are useful in detecting localised gear faults, however they are of little value in determining the type of fault.

3. The Narrow Band technique has improved sensitivity over FM4 in the early stages of damage.

4. FM4 appears to be a better discriminator of the extent of damage than the Narrow Band technique.

The techniques described above are all based on the time domain representation of the signal average. One problem noted was that there was limited discrimination in the type of fault. Another problem with these techniques is that they require selective filtering of the signal average. In order to do this, we must assume certain properties of the signal average (e.g. what constitutes the 'regular' signal). This may not always be as simple as it would appear and, as will be shown later, some of the assumptions made in the previous section were in fact incorrect.

Ideally, we would like to be able to represent the signal average in such a way that it

(a) requires no filtering and

(b) enables the discrimination of fault type as well as detection of the presence of a fault.

In the following sections, a representation of the signal average as a distribution of energy simultaneously in time and frequency is investigated as a means of meeting the two requirements listed above.

5. TIME-FREQUENCY DISTRIBUTIONS.

The basic goal of a joint time-frequency distribution is to provide a representation of the energy or intensity of a signal simultaneously in time and frequency. For a time based signal s(t), the instantaneous energy (intensity per unit time) is the absolute value of the signal squared,

$$|s(t)|^2 = \text{intensity per unit time at time t.} \tag{1}$$

The energy density spectrum (intensity per unit frequency) is the absolute value of the Fourier transform squared,

$$|S(f)|^2 = \text{intensity per unit frequency at frequency f} \tag{2}$$

where S(f) is the Fourier transform of s(t)

$$S(f) = \int_{-\infty}^{+\infty} s(t)\, e^{-j2\pi ft}\, dt \tag{3}$$

A joint time-frequency distribution P(t,f) should represent the intensity per unit time per unit frequency at time t and frequency f,

$$P(t,f) = \text{intensity at time t and frequency f} \tag{4}$$

Ideally the summation of P(t,f) for all frequencies at a particular time would give the instantaneous energy (1), and the summing up over all times at a particular frequency would give the energy density spectrum (2),

$$\int_{-\infty}^{+\infty} P(t,f)\, df = |s(t)|^2 \tag{5}$$

$$\int_{-\infty}^{+\infty} P(t,f)\, dt = |S(f)|^2 \tag{6}$$

Equations 5 and 6 are termed the 'marginals' and are conditions which should be met by a time-frequency distribution.

6. THE WIGNER-VILLE DISTRIBUTION.

One distribution which meets the marginals is the Wigner-Ville distribution.

6.1 History.

The Wigner distribution was first introduced in the field of quantum mechanics in 1932 by Wigner [6]. The formulation used here, the Wigner-Ville distribution, was first proposed as a tool for signal analysis in 1948 by Ville [7]. This formulation combines the analytic signal with the Wigner distribution and has a number of advantages over the Wigner distribution in signal analysis [4]. Interest in its application to a number of signal processing requirements has increased over the last decade, particularly where non-stationary signals are involved.

A number of interesting applications of the Wigner-Ville distribution (WVD) have be reported, including speech recognition, electrocardiogram interpretation, seismic studies and oceanography [4,8,9,10].

6.2 Definition.

For the analytic signal s(t), the Wigner-Ville Distribution W(t,f) is defined as [4]:

$$W(t,f) = \int_{-\infty}^{+\infty} s(t+\tau/2)s^*(t-\tau/2)e^{-j2\pi f\tau}\, d\tau \qquad (7)$$

where $s^*(t)$ is the complex conjugate of s(t).

The analytic signal s(t) is derived from a real signal x(t) by setting the imaginary part equal to the Hilbert transform of x(t):

$$s(t) = x(t) + jH[x(t)], \qquad (8)$$

The Hilbert transform H[x(t)] is defined as [11]:

$$H[x(t)] = \frac{1}{\pi} \int_{-\infty}^{+\infty} \frac{x(v)}{t-v} dv \tag{9}$$

The distribution W(t,f) is real-valued for all t and f, but is not necessarily positive.

6.3 Discrete-Time/Frequency Wigner-Ville Distribution.

Let $\hat{x}(t)$ be a discrete version of the continuous time signal x(t). Where the sample interval in time is T and we limit the number of samples to N, the relationship between $\hat{x}$ and x can be expressed as,

$$\hat{x}(t) = \sum_{n=0}^{N-1} x(nT)\, \delta(t-nT) \tag{10}$$

The signal $\hat{x}(t)$ is periodic in an interval of length NT which leads to a discrete spectrum with a sample interval Λ in frequency of

$$\Lambda = \frac{1}{NT} \tag{11}$$

The discrete analytic signal $\hat{s}(t)$,

$$\begin{aligned} \hat{s}(t) &= \hat{x}(t) + jH[\hat{x}(t)] \\ &= \sum_{n=0}^{N-1} s(nT)\, \delta(t-nT) \end{aligned} \tag{12}$$

can be easily obtained from $\hat{x}(t)$ using the discrete Fourier transform [11]

$$\hat{S}(f) = \begin{cases} 0, & f < 0 \\ \hat{X}(f), & f = 0 \\ 2\hat{X}(f), & f > 0 \end{cases} \tag{13}$$

where $\hat{S}(f)$ and $\hat{X}(f)$ are the discrete Fourier transforms of $\hat{s}(t)$ and $\hat{x}(t)$ respectively. The inverse Fourier transform of $\hat{S}(f)$ gives $\hat{s}(t)$.

The Wigner-Ville distribution of $\hat{s}(t)$, $W_{\hat{s}}(t,f)$, can be derived [12] by inserting (12) into (7),

$$W_{\hat{s}}(t,f) = \int_{-\infty}^{+\infty} \left[\sum_{k=0}^{N-1} s(kT)\,\delta(t+\tau/2-kT) \right] \cdot \left[\sum_{n=0}^{N-1} s^*(nT)\,\delta(t-\tau/2-nT) \right] e^{-j2\pi f\tau}\, d\tau \tag{14}$$

$$= \frac{1}{N} \sum_{n=0}^{N-1} \sum_{k=0}^{N-1} s(kT)s^*(nT)\, e^{-j2\pi f(k-n)T}\, \delta(t-(k+n)T/2) \tag{15}$$

which can be put into the form:

$$W_{\hat{s}}(t,f) = \frac{1}{2N} \sum_{n=0}^{2N-1} \sum_{k=0}^{N-1} s(kT)s^*((n-k)T)\, e^{-j2\pi f(2k-n)T}\, \delta(t-nT/2) \tag{16}$$

Note that the WVD of the sampled signal, $W_{\hat{s}}(t,f)$, is sampled at half the interval (T/2) of the signal and has a period of 2NT - giving a sample interval in frequency for $W_{\hat{s}}(t,f)$ of 1/(2NT):

$$W_{\hat{s}}(t,f) = \frac{1}{2N} \sum_{n=0}^{2N-1} \sum_{k=0}^{N-1} \sum_{m=0}^{2N-1} s(kT)s^*((n-k)T)\, e^{-j2\pi m(2k-n)/N}\, \delta(t-nT/2)\delta(t-m/2NT) \tag{17}$$

The discrete-time/frequency WVD, $\hat{W}(n,m)$, can be defined as the weight of the bidimensional Dirac function at the points t = nT/2 and f = m/2NT

$$\hat{W}(n,m) = \frac{1}{2N} \sum_{k=0}^{N-1} s(kT)\, s^*((n-k)T)\, e^{-j\pi m(2k-n)/N} \tag{18}$$

where $0 \le n \le 2N-1$ and $0 \le m \le 2N-1$.

$\hat{W}(n,m)$ can be easily computed using the fast Fourier transform (FFT) algorithm. For the even time samples, (18) becomes:

$$\hat{W}(2n,m) = \frac{1}{2N} \sum_{k=0}^{N-1} s(kT)\, s^*((2n-k)T)\, e^{-j2\pi m(k-n)/N} \tag{19}$$

and for the odd time samples:

$$\hat{W}(n,m) = \frac{1}{2N} e^{-j\pi m/N} \sum_{k=0}^{N-1} s(kT)\, s^*((2n-k+1)T)\, e^{-j2\pi m(k-n)/N} \tag{20}$$

6.4 Implementation.

In this paper the Wigner-Ville is applied to the signal average which is exactly periodic within its window. This allows the discrete Wigner-Ville distribution as described above to be easily implemented. Where the terms in s(n) fall outside the window, a simple modulus function is used (i.e. the (n+N)th sample of a N sample average is equivalent to the (n)th sample).

6.5 Visual Representation.

The Wigner-Ville distribution of a signal can be represented in a number of ways. For the purpose of this study, colour has been used to represent the amplitude of the signal. The logarithmic amplitude has been divided into twelve contour levels, each represented by a colour. A minimum level has been set, below which no contours are plotted.

In all the examples the maximum value of each distribution has been set to 0dB, with all other levels scaled accordingly. It is important to note that we are not concerned with the absolute signal levels here, but rather the pattern produced by various signal types.

7. NUMERICAL EXAMPLES.

Before looking at practical examples of vibration signals, the WVDs of some synthesized signals are studied, which give a guide to the interpretation of signal types.

All examples simulate signals from a rotating source which is periodic in the window. The axes are given as rotation of the source (0 to 360 degrees) and orders[2]

---

[2] orders = cycles per revolution.

which are proportional to time and frequency respectively for machinery rotating at constant speed.

The graphs include the original signal and its logarithmic spectrum for comparison with the calculated WVD.

7.1 Stationary Signals.

Figure 1 shows the WVD of a single continuous sine wave of 22 orders. As would be expected, this produces a single line of constant amplitude.

In Figure 2, a second continuous sine wave of 44 orders has been added to the 22 order signal. This produces a second line at 44 orders. However, another (broken) line has appeared at 33 orders. This is a property of the WVD, which produces zero energy cross-terms at frequencies $(f1+f2)/2$ of signals composed of the sum of two sine waves at frequencies f1 and f2. This property can be useful in the interpretation of signals, as it gives an indication that two parallel signals exist. It can also be misleading if one is not aware of this phenomenon.

7.2 Modulated Signals.

Figure 3 shows the WVD of a signal in which the frequency varies between 21 and 23 orders in a cyclic fashion. Such a variation might result, for example, from an eccentricity in the rotating assembly.

Figure 4 shows a 22 order signal with amplitude varying between 1 and 0 units in a cyclic fashion.

A signal of 22 orders combining the frequency and amplitude modulations seen in Figures 3 and 4 produces the WVD shown in Figure 5. Both modulations are clearly detectable in the WVD but are difficult to interpret in either the original signal or its spectrum.

7.3 Short term changes.

A number of faults encountered in gearboxes will produce only momentary changes in the vibration signal. Such faults include tooth damage on gears, such as cracks, pitting, and spalling.

Figure 6 shows the WVD of a 22 order signal containing a momentary phase lag in the eleventh cycle. As can be seen from the original signal and its spectrum, this type of signal variation is difficult to interpret with single domain representations but presents a striking pattern in the WVD.

In Figure 7, an amplitude drop has been added to the phase lag on the eleventh cycle. The WVD again shows a striking pattern, but clearly distinguishable from that in Figure 6. The time signal shows the amplitude drop clearly, but the phase lag is barely detectable. The frequency spectrum is difficult to interpret.

Figure 8 shows a 22 order signal in which the eleventh cycle has an amplitude 1.5 times higher than the other cycles.

7.4 Impacts.

In practice, it would be expected that an impact would excite resonances within the mechanical structure. Figure 9 shows the signal portrayed in Figure 7 with a simulated resonance at 12 orders added. This has been done by including a signal burst of 12 orders commencing at the tenth cycle (of the 22 order signal) and having an exponential decay.

8. PRACTICAL EXAMPLES.

In this section, the Wigner-Ville Distribution is applied to the six examples described in Section 3.

Note that in all examples the datum angle of rotation does not necessarily start at the same point and should only be used to indicate the relative position of features within a single plot.

8.1 Wessex Input Pinion.

8.1.1 Undamaged Pinion.

Figure 10 shows the WVD for the signal average of the undamaged Wessex input pinion. The major meshing components can be seen at 22 and 66 orders, with a smaller component at 44 orders which also includes a contribution due to the cross-products of the 22 and 66 order components. Cross-products can also be seen at 33 and 55 orders. Other patterns can be seen which indicate minor variations in the meshing action of the gear. These variations are normal and can be clearly distinguished from gear faults as will be seen later.

8.1.2 Wessex Input Pinion Fatigue Crack.

By applying the WVD to the signal average of the cracked pinion, we can clearly detect the aberration in the vibration at 263.4 and 324.3 hours since overhaul (103 and 42 hours before failure respectively) in Figures 11 and 12. The features seen in these plots, are similar to those seen in Figure 9 for a signal with a phase lag, corresponding

amplitude drop and a resonance excited by an impact. It was shown in [13] that these are the characteristic features of a cracked bevel gear.

It should be noted that these WVDs are not for the same gear as that shown in Figure 10 and, therefore, the relative magnitudes of the mesh components at 22, 44, 66 and 88 orders should not be directly compared. This particular gear has major mesh components at 44 and 88 orders rather than at 22 and 66 orders for the gear in Figure 10; it is thought that the different location of the major mesh harmonics is not an indication of damage.

One additional feature of interest seen in these figures is the vertical line at 25 orders. This is not the meshing frequency, which appears at 22 orders. This 25 order frequency had previously been noted in [2] and [14] and been attributed as '...either a ghost component arising from transmission errors introduced during the machining of the gear, or else the third upper sideband of the fundamental meshing frequency.' Its appearance in the Wigner-Ville as constant in time eliminates the possibility of it being a sideband, although not confirming that it is a ghost frequency.

8.1.3 Wessex Input Pinion Micro-Pitting.

Figure 13 shows the WVD of the signal average of the Wessex input pinion which had severe micro-pitting (frosting) of the tooth surfaces.

In this WVD, we can clearly see evidence of a fault centred about 140 degrees of rotation on the diagram. The pattern is clearly distinguishable from those for the cracked pinion seen in Figures 11 and 12. It is important to note that although the major meshing component (vertical red line) appears at 22 orders in this case and at 44 orders in the case of the cracked pinion, this is not thought to be of great significance in the analysis of the fault.

8.2 Epicyclic Test Rig Planet Gear.

8.2.1 Undamaged Planet.

Figure 14 shows the WVD of the signal average of an undamaged planet gear. As with the undamaged Wessex input pinion, we see components at the meshing harmonics (32, 64 and 96 orders in this case), cross-products and patterns due to minor variations in meshing action.

8.2.2 Damaged Planet.

The WVD of the signal average of the damaged planet is shown in Figure 15. The pattern produced by the damaged tooth is clearly seen at around 250 degrees of rotation. Note that there is some similarity between this figure and Figure 11 of the cracked Wessex input pinion 103 hours before failure. This would be caused by teeth not taking up their share of the load in both cases, due to the reduction in stiffness in the tooth adjacent to the crack in the case of the Wessex input pinion, and improper meshing of the ground tooth in the case of the planet gear.

Note that the evidence of damage here is seen about the 32 order line, which in this case is not the dominant meshing harmonic. Although not obvious in Figure 15 due to the use of a logarithmic scale, the 64 order line is the dominant meshing harmonic.

9. RAMIFICATIONS FOR APPLICATION OF EXISTING TECHNIQUES.

In Section 4, a number of assumptions were made about the nature of the signal averages which, as stated in 4.3, were incorrect in some cases.

9.1 Cracked Wessex Input Pinion.

In 8.1.2, we noted that there appeared to be a 25 order 'ghost' frequency in the signal average of the cracked input pinion. In this case, this would constitute part of the 'regular' signal as it is part of the normal vibration for the shaft (due to profile errors - which do not constitute a gear 'fault').

The FM4 analyses for the cracked input pinion were repeated including 25 orders as part of the 'regular' signal. This gave a result of 4.77 at 103 hours before failure and 6.05 at 42 hours before failure compared to 4.16 and 5.96 respectively using our original assumptions. This would have changed our damage level indicator at 103 hours before failure from a 'warning' to 'danger' level.

9.2 Damaged Planet Gear.

In 8.2.2 it was noted that the evidence of damage was centred around the 32 order line and not the dominant mesh harmonic at 64 orders. In the Narrow Band technique, the dominant meshing harmonic is used as a centre frequency.

The Narrow Band technique for the damaged planet gear was repeated using 32 orders as our centre frequency. This gave a level of 8.81, a startling contrast to our original level of 3.68.

10. CONCLUSIONS.

The preliminary studies outlined have indicated that the WVD shows great promise as a tool for the detection and discrimination of gear faults. Traditional vibration analysis methods require selective use and do not necessarily distinguish the type or extent of a fault. A number of these methods require the removal of a large portion of the signal in order to highlight small variations in the meshing action of the gear. Incorrect selection of the signal components to be removed can result in misleading diagnosis.

In addition to its use as a diagnostic tool, the examples given have shown that the additional information about the nature of the signal provided by the Wigner-Ville distribution can be used to refine the application of existing techniques; in some cases with dramatic improvement in performance.

The computational requirements of the WVD and the need for knowledgeable interpretation of the results are likely to confine its use to the laboratory for the time being. However, the ability to portray the full content of the vibration signal in a single function may provide a suitable platform for an automated fault detection system using pattern recognition techniques.

The ability of the WVD to provide relatively high resolution representations of short term non-stationary signals in both time and frequency indicate that it may be of considerable use in other areas of machinery health monitoring, such as the study of engine vibration data, particularly over rapid engine run-up and run-downs where the resolution provided by techniques such as short-term FFTs may be insufficient.

REFERENCES.

[1] Randall, R.B., "A New Method of Modelling Gear Faults", Trans. ASME, J. Mech. Design, Vol. 104, pp. 259-267, 1982.

[2] McFadden, P.D. and Smith, J.D., "A Signal Processing Technique for Detecting Local Defects in a Gear from the Signal Average of the Vibration", Proceedings of the Institute of Mechanical Engineers, Vol 199, Part C, No. 4, pp 287-292, 1985.

[3] Stewart, R.M., "Some Useful Data Analysis Techniques for Gearbox Diagnostics", I.S.V.R., Univ. of Southampton, Report MHM/R/10/77, July 1977.

[4] Boashash, B., "Non-Stationary Signals and the Wigner-Ville Distributions: A Review", IASTED International Symposium on Signal Processing and its Applications - ISSPA 87, Brisbane, vol. 1, pp. 261-268, August 1987.

[5] McFadden, P.D., "Examination of a Technique for the Early Detection of Failure in Gears by Signal Processing of the Time Domain Average of the Meshing Vibration", ARL Aero Propulsion Technical Memorandum 434, 1986.

[6] Wigner, E.P., "On the Quantum Correction for Thermodynamic Equilibrium", Phys. Review., vol. 40, pp. 749-759, 1932.

[7] Ville, J., "Theorie et Applications de la notion de Signal Analytique", Cables et Transmission, vol. 194, no. 1, pp. 61-74, 1948.

[8] Boashash, B. and Abeysekera, S.S., "Two-dimensional processing of speech and ECG signals using the Wigner-Ville distribution", Proceedings of the International Society for Optical Engineering, Vol. 697, Applications of Digital Image Processing IX, pp. 142-153, 1986.

[9] Boashash, B. and Whitehouse, H.J., "Seismic applications of the Wigner-Ville Distribution", Proceedings of the 1986 IEEE International Circuits and Systems Symposium, Vol. 1, pp. 34-37, San Jose, USA, May 1986.

[10] Imberger, J., "Signal Processing requirements in Oceanography", IASTED International Symposium on Signal Processing and its Applications - ISSPA 87, Brisbane, vol. 1, pp. 8-9, August 1987.

[11] Bendat, J.S., "The Hilbert Transform and Applications to Correlation Measurements", Bruel and Kjaer, Copenhagen.

[12] Peyrin, F. and Prost, R., "A Unified Definition for the Discrete-Time, Discrete-Frequency, and Discrete-Time/Frequency Wigner Distributions', IEEE Tans. on Acoustics, Speech, and Signal Processing, Vol. 34, No. 4, pp. 858-866, August 1986.

[13] McFadden, P.D., "Detecting Fatigue Cracks in Gears by Amplitude and Phase Demodulation of the Meshing Vibration", Trans. of the ASME, Journal of Vibration, Acoustics, Stress and Reliability in Design, Vol. 108, pp. 165-170, April 1986.

[14] McFadden, P.D., "Analysis of the Vibration of the Input Bevel Pinion in RAN Wessex Helicopter Main Rotor Gearbox WAK143 Prior to Failure", ARL Aero Propulsion Report 169, September 1985.

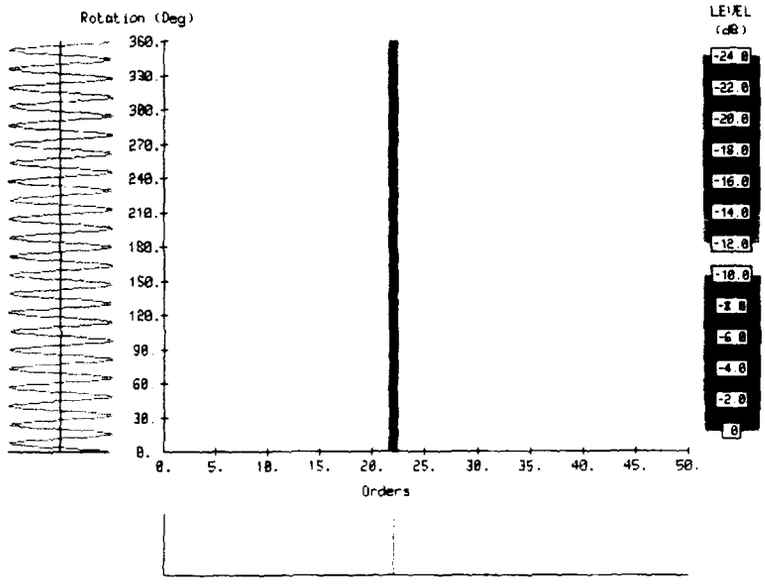

Figure 1. **Single Stationary signal**

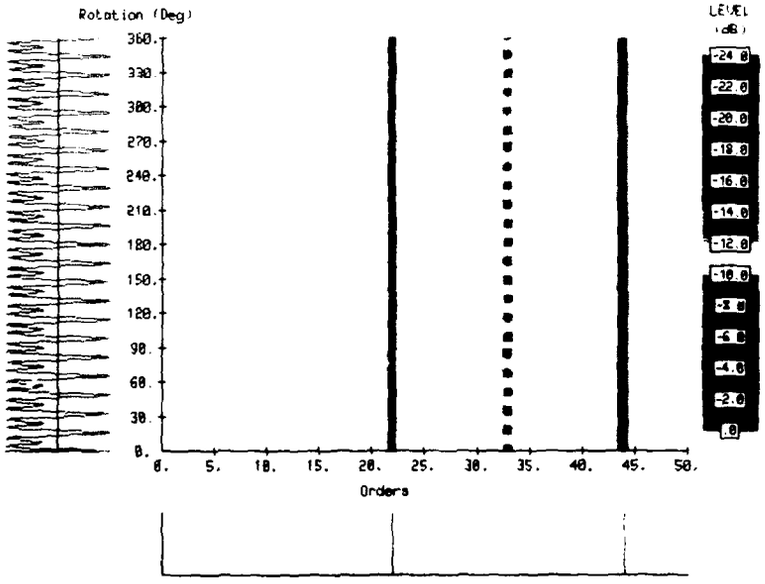

Figure 2. **Multiple Stationary Signals.**
Showing zero energy crossproduct (only positive part plotted)

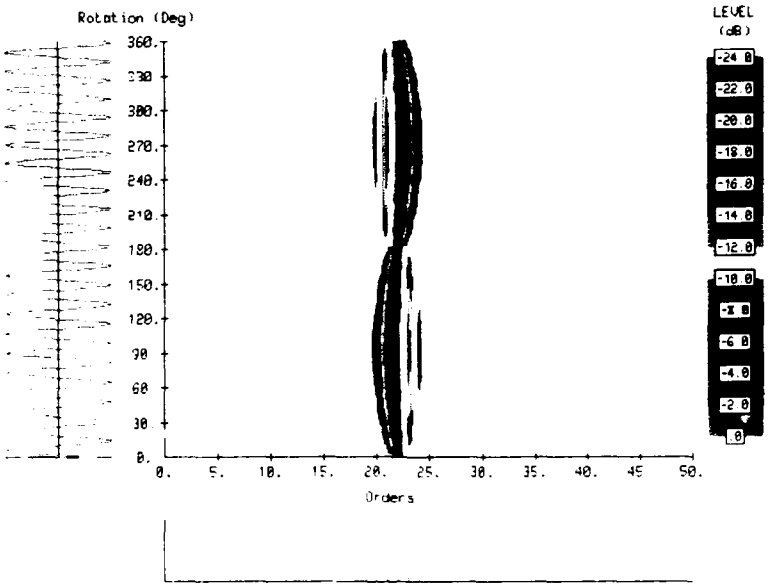

Figure 3. **Cyclic frequency modulated signal.**
Could be caused by eccentricity in shaft or gearwheel.

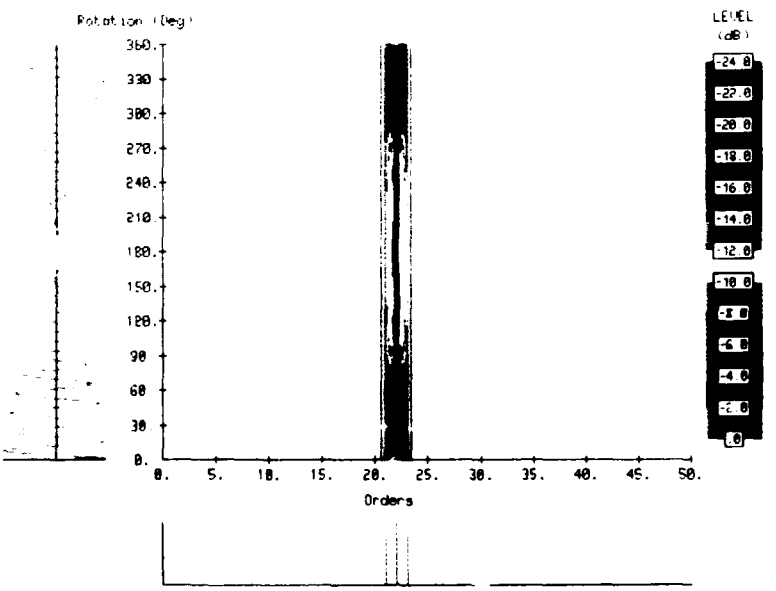

Figure 4. **Cyclic amplitude modulated signal.**

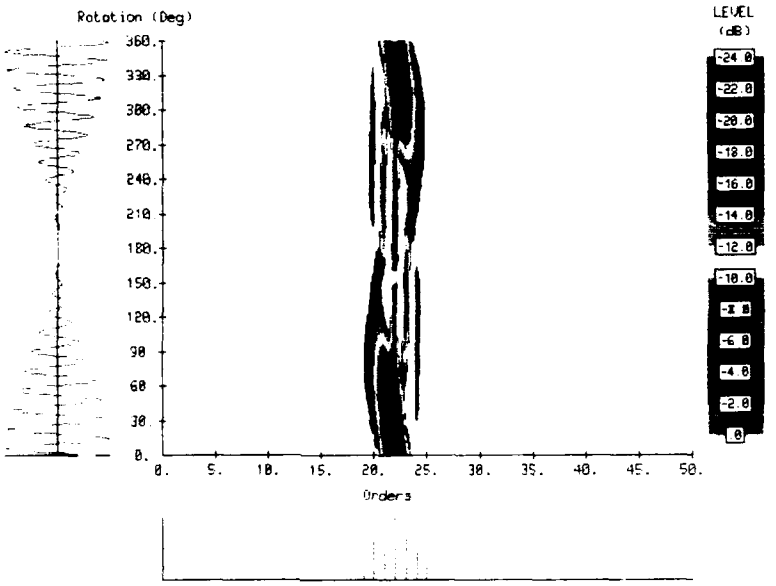

Figure 5. **Combined amplitude and frequency modulation.**

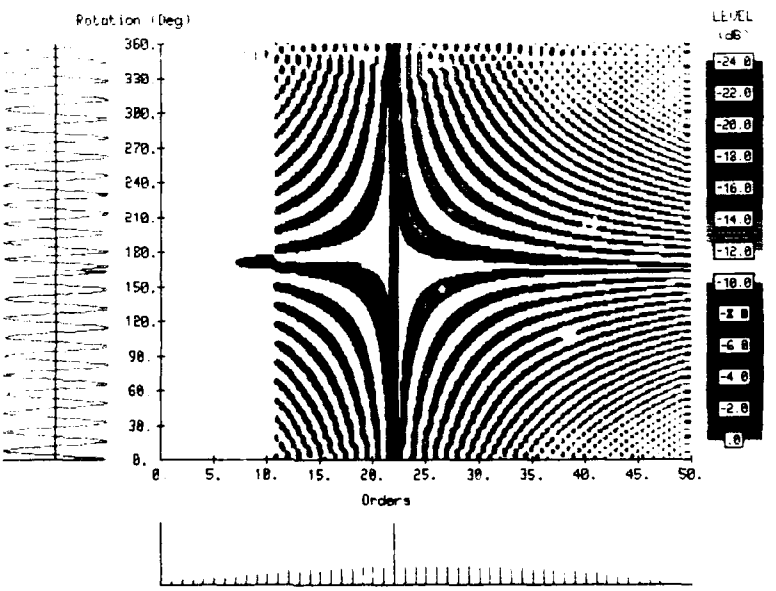

Figure 6. **Short term phase change.**

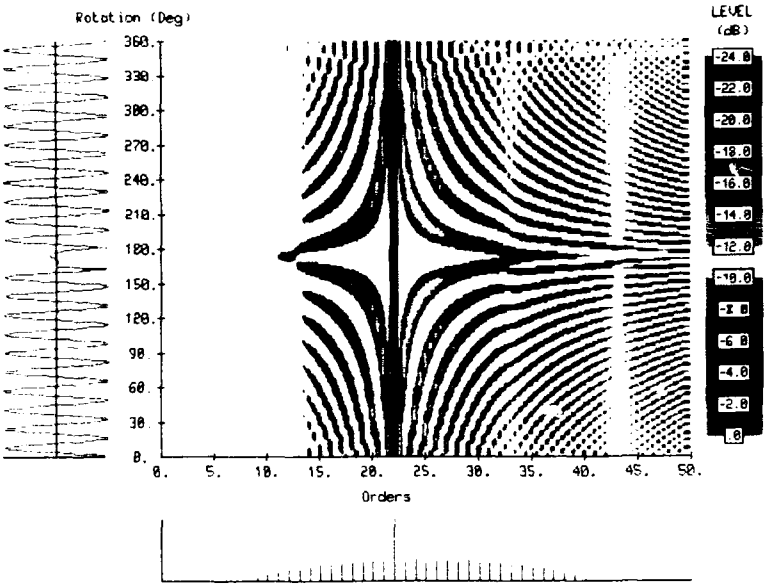

Figure 7. Short term amplitude and phase change. Could be caused by chipped or cracked tooth.

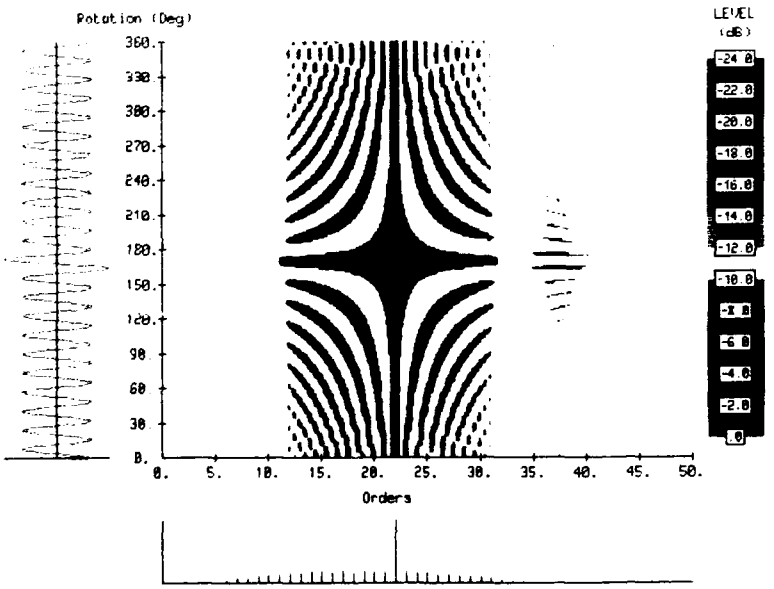

Figure 8. Short term amplitude increase. Could be caused by tooth surface damage (e.g. spalling).

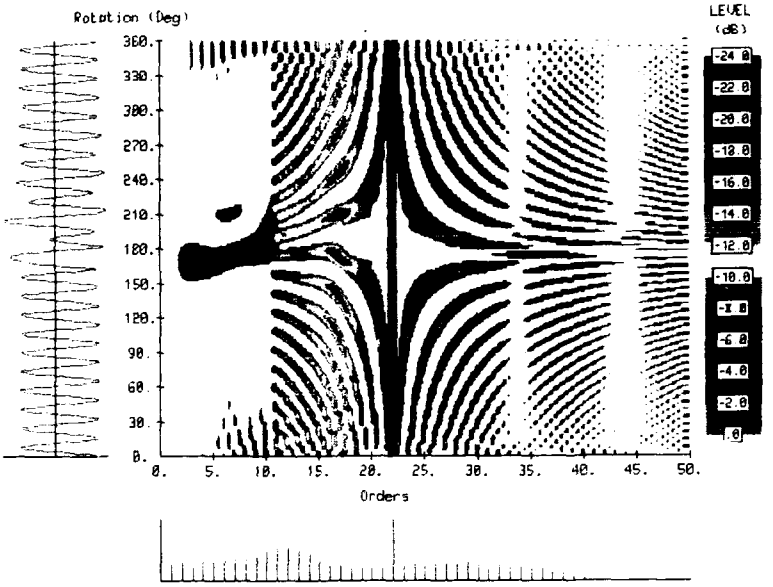

Figure 9. **Short term amplitude and phase change with decaying resonance. Could be caused by advanced tooth crack, giving impact.**

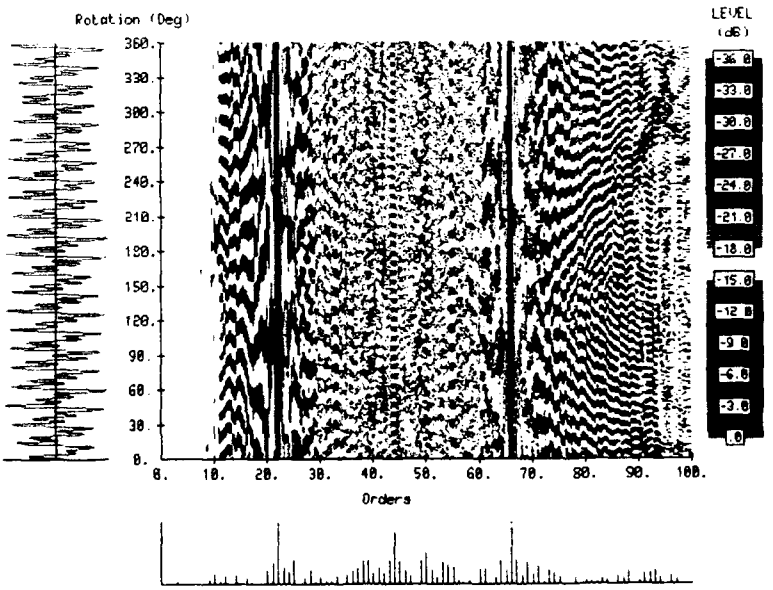

Figure 10. **Normal Wessex Input Pinion.**

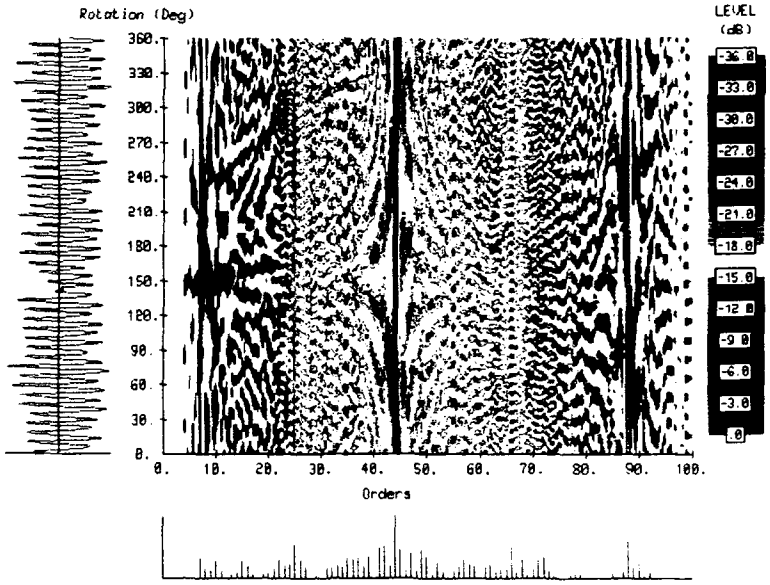

Figure 11. **Cracked Wessex Input Pinion (103 Hours before failure).**

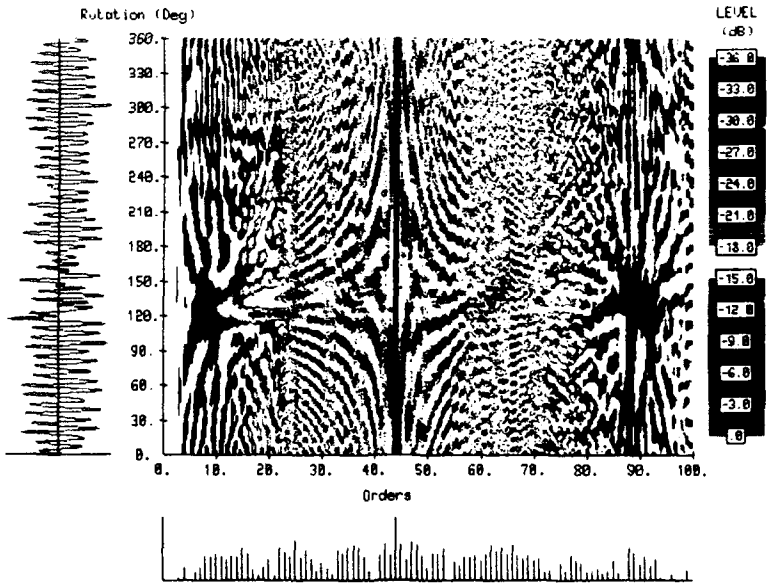

Figure 12. **Cracked Wessex Input Pinion (42 Hours before failure).**

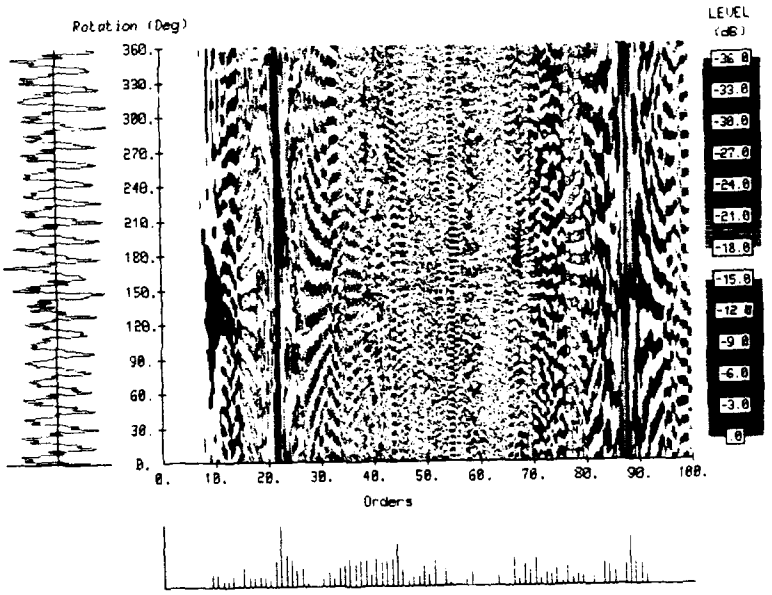

Figure 13. **Wessex Input Pinion with micro-pitting.**

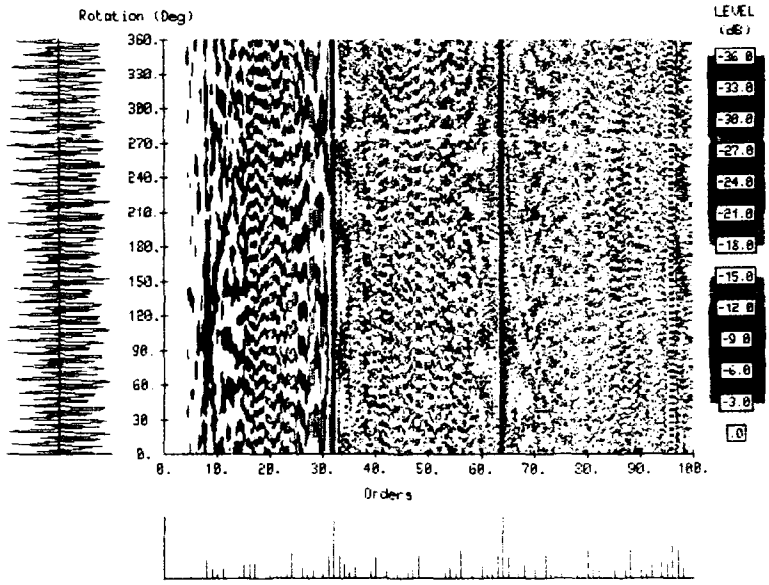

Figure 14. Undamaged Epicyclic Planet Gear.

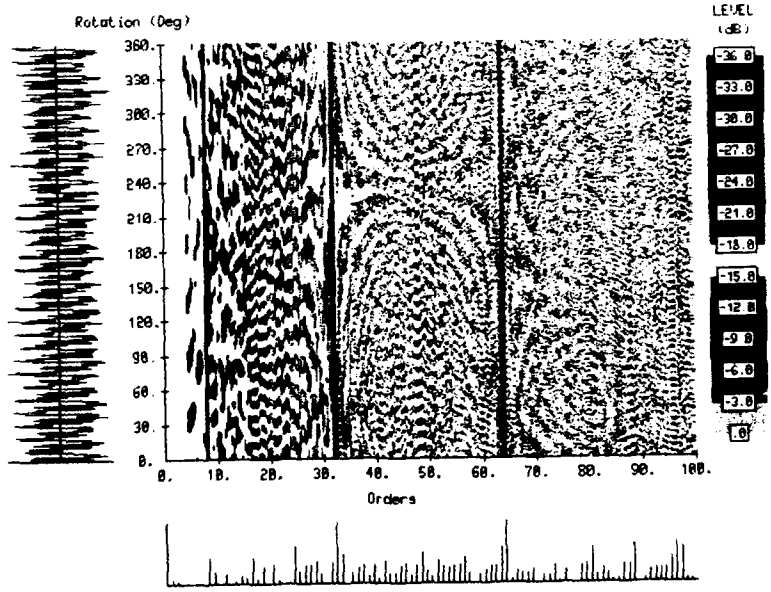

Figure 15. Damaged Epicyclic Planet Gear.

DISTRIBUTION

AUSTRALIA

Department of Defence

Defence Central
- Chief Defence Scientist)
- AS, Science Corporate Management) shared copy
- FAS Science Policy)
- Director, Departmental Publications
- Counsellor, Defence Science, London (Doc Data sheet only)
- Counsellor, Defence Science, Washington (Doc Data sheet only)
- S.A. to Thailand MRD (Doc Data sheet only)
- S.A. to the DRC (Kuala Lumpur) (Doc Data sheet only)
- Scientific Adviser, Defence Central
- OIC TRS, Defence Central Library
- Document Exchange Centre, DSTIC (8 copies)
- Defence Intelligence Organisation
- Librarian H Block, Victoria Barracks, Melbourne (Doc Data sheet only)
- Defence Industry and Materiel Policy, FAS

Aeronautical Research Laboratory
- Director
- Library
- Chief Flight Mechanics and Propulsion Division
- Branch File - Propulsion
- Author: B.D. Forrester
- B. Rebbechi
- N.S. Swansson
- S. Henbest
- I.M. Howard

Materials Research Laboratory
- Director/Library

Defence Science & Technology Organisation - Salisbury
- Library

WSRL
- Maritime Systems Division (Salisbury), Dr R.F. Barrett

Navy Office
- Navy Scientific Adviser (3 copies)
- Aircraft Maintenance and Flight Trials Unit
- Director of Aircraft Engineering - Navy
- Naval Support Command
  - Superintendent, Naval Aircraft Logistics
- Directorate of Aviation Projects - Navy
- Director of Naval Supply - Aviation & Major Projects

Army Office
Scientific Adviser - Army (Doc Data sheet only)
Engineering Development Establishment Library
US Army Research, Development and Standardisation Group

Air Force Office
Air Force Scientific Adviser (Doc Data sheet only)
Aircraft Research and Development Unit
Scientific Flight Group
Engineering Branch Library
HQ Logistics Command (DGELS)

Department of Transport & Communication
Library

Statutory and State Authorities and Industry
Civil Aviation Authority

Universities and Colleges
Adelaide
Barr Smith Library

Melbourne
Engineering Library

Monash
Hargrave Library
Dr J. Mathews

Newcastle
Library
Professor R. Telfer, Institute of Aviation

Sydney
Engineering Library

NSW
Physical Sciences Library
Library, Australian Defence Force Academy

Queensland
Library

Queensland University of Technology
Prof B. Boashash

Swinburne Institute of Technology
Dr I. Freshwater

Western Australia
Library

RMIT
Library

University College of the Northern Territory
Library

CANADA
International Civil Aviation Organization, Library

NRC
J.H. Parkin Branch (Aeronautical & Mechanical Engineering Library)
Canada Institute for STI

NETHERLANDS
National Aerospace Laboratory (NLR), Library

NEW ZEALAND
Defence Scientific Establishment, Library
RNZAF
Transport Ministry, Airworthiness Branch, Library

UNITED KINGDOM
Ministry of Defence, Research, Materials and Collaboration
Defence Research Agency (Aerospace)
Bedford, Library
Pyestock, Director
Commonwealth Air Transport Council Secretariat
Defence Research Agency (Naval)
Holton Heath, Dr N.J. Wadsorth
St Leonard's Hill, Superintendent
NAML, Mr Peter Gadd,
British Library, Document Supply Centre
Aircraft Research Association, Library
Rolls-Royce Ltd, Aero Division Bristol, Library
Civil Aviation Authority

Universities and Colleges

Cambridge
Library, Engineering Department
Whittle Library

London
Head, Aero Engineering

Oxford
Dr P.D. McFadden

Southampton
Library
Prof J. Hammond, ISVR

Cranfield Inst. of Technology
Library
Dr R.H. Bannister, School of Mechanical Engineering

Imperial College
Aeronautics Library

UNITED STATES OF AMERICA
NASA Scientific and Technical Information Facility
NASA Lewis Research Center, Mr J. Zakrajsek
United Technologies Corporation, Library
McDonnell Aircraft Company, Library
Nondestructive Testing Information Analysis Center

Universities and Colleges

Princeton
Head, Mechanics Department

Massachusetts Inst. of Technology
MIT Libraries

SPARES (25 COPIES)

TOTAL (115 COPIES)

AL 149 DEPARTMENT OF DEFENCE

DOCUMENT CONTROL DATA

PAGE CLASSIFICATION
UNCLASSIFIED

PRIVACY MARKING

1a. AR NUMBER	1b. ESTABLISHMENT NUMBER	2. DOCUMENT DATE	3. TASK NUMBER
AR-005-606	ARL-PROP-R-180	AUGUST 1991	DST 89/089

4. TITLE
TIME-FREQUENCY DOMAIN ANALYSIS OF HELICOPTER TRANSMISSION VIBRATION

5. SECURITY CLASSIFICATION (PLACE APPROPRIATE CLASSIFICATION IN BOX(S) IE. SECRET (S), CONF. (C) RESTRICTED (R), UNCLASSIFIED (U)).

DOCUMENT	TITLE	ABSTRACT
U	U	U

6. NO. PAGES
29

7. NO. REFS.
14

8. AUTHOR(S)
B.D. FORRESTER

9. DOWNGRADING/DELIMITING INSTRUCTIONS
Not applicable

10. CORPORATE AUTHOR AND ADDRESS
AERONAUTICAL RESEARCH LABORATORY
506 LORIMER STREET
FISHERMENS BEND VIC 3207

11. OFFICE/POSITION RESPONSIBLE FOR:
SPONSOR DSTO
SECURITY -
DOWNGRADING -
APPROVAL DARL

12. SECONDARY DISTRIBUTION (OF THIS DOCUMENT)
Approved for public release

OVERSEAS ENQUIRIES OUTSIDE STATED LIMITATIONS SHOULD BE REFERRED THROUGH DSTIC, ADMINISTRATIVE SERVICES BRANCH, DEPARTMENT OF DEFENCE, ANZAC PARK WEST OFFICES, ACT 2601

13a. THIS DOCUMENT MAY BE ANNOUNCED IN CATALOGUES AND AWARENESS SERVICES AVAILABLE TO . . . .
No limitations

13b. CITATION FOR OTHER PURPOSES (IE. CASUAL ANNOUNCEMENT) MAY BE [X] UNRESTRICTED OR [ ] AS FOR 13a.

14. DESCRIPTORS
Vibration measurement
Frequency analyzers
Time domain
Transmissions (mechanical)

15. DISCAT SUBJECT CATEGORIES
010301

16. ABSTRACT
Vibration Analysis is playing an increasingly important role in the early detection of helicopter transmission faults. Current vibration analysis techniques used in helicopter transmission fault detection require selective filtering or manipulation of the signal, based on assumptions about the nature of the signal. In some cases these techniques can give misleading results. It is shown that the application of time-frequency domain representations, based on the Wigner-Ville distribution, is capable of detecting a variety of vibration features which can be used to classify faults.

PAGE CLASSIFICATION
PRIVACY MARKING

THIS PAGE IS TO BE USED TO RECORD INFORMATION WHICH IS REQUIRED BY THE ESTABLISHMENT FOR ITS OWN USE BUT WHICH WILL NOT BE ADDED TO THE DISTIS DATA UNLESS SPECIFICALLY REQUESTED.

16. ABSTRACT (CONT).

17. IMPRINT

AERONAUTICAL RESEARCH LABORATORY, MELBOURNE

18. DOCUMENT SERIES AND NUMBER	19. COST CODE	20. TYPE OF REPORT AND PERIOD COVERED
Propulsion Report 180	43 414A	

21. COMPUTER PROGRAMS USED

22. ESTABLISHMENT FILE REF.(S)

23. ADDITIONAL INFORMATION (AS REQUIRED)